

# **Estimating Dynamic properties of long bones under impact bending using inverse finite element method**

**Mike W J Arun, Anoop Chawla, Sudipto Mukherjee**

## **1. ABSTRACT**

The objective of this work is to formulate a material model for bone, which can predict stresses and fracture for wide range of strain rates. Impactor force-data recorded in 3-pt bending impact tests on human humerus was used. A total of twelve samples were tested at impact velocities of 3.23, 4.43 and 5.42 m/s. Detailed FE mesh of the specimen was obtained using CT scans. In order to capture the non-homogeneity of the material, the mesh was divided into twenty material sets based on Hounsfield Number from CT Scans and material properties were assigned to them. A user defined material model was developed that incorporates the rate dependency of stiffness, yielding and failure. A Drucker-Prager plastic model was chosen as it captures dilation of bone and asymmetry in yielding. A phenomenological damage model was chosen to capture the shear failure mechanism. The sums of the errors between the simulation and the experimental result for the three drop heights were minimized using constrained Genetic Algorithm. A single material model was thus obtained that well predicts the result (correlation >0.9) in all cases. A logarithmic relation was used to model strain-rate dependency of elastic modulus, yield and damage initiation. The quasistatic modulus of bone is found to vary between 0.7 and 6 Gpa for cancellous and between 7 and 19 Gpa for cortical bone. For bone with Hounsfield Number of 1600 the modulus is found to vary from 19 to 50 Gpa as strain rate varies from 0.001 to 300/s.

## **2. INTRODUCTION**

Human body organs like any other structures develop internal forces when external forces are applied. These internal forces try to restore the organ's original shape and size. But these internal forces (or stresses) are limited, after which the organ fails. To prevent injuries it is very important to understand the forces and the mechanisms that are causing the injuries. In biomechanics literature this is done in three ways, experimentally traumatizing cadavers [1], using Anthropomorphic Test Devices (ATD or commonly known as dummies)[2] and using Finite Element Models [3]. Generally information from cadaver experiments is used to validate both ATDs and finite element models. Nearly 30% of the cost of a consumer vehicle can be traced back to engineering and testing efforts [4]. Automakers are trusting in the ability of math-based simulation tools to reduce engineering costs, hence increasing profits. Safety testing is a very expensive business, as millions of dollars of space and equipment are needed to perform experiments. Validated finite element (FE) models facilitate to move away from expensive laboratory tests toward cost efficient math-based simulations. These FE models help to perform research in places where sophisticated labs are not present, especially in developing countries. For the purpose three types of validated finite element models are generally required, namely vehicle model, dummy model and human body model. To have an accurate human body model, it is necessary to have accurate FE models of human body parts. The aim of this work is to develop a finite element model for long bones, which will predict the response including fracture that are observed in laboratory experiments.

### 3. MATERIALS AND METHOD

#### 3.1. Experiment

Twelve isolated human humerus were collected through All India Medical Sciences, India. All specimens were tested in three point bending mode in the anterior to posterior direction. An instrumented drop tower was used to impact the bone. The drop tower consists of a carriage of mass 31 kg that can fall freely through guided slots. The height of the carriage can be adjusted to vary impact velocity. A strain gauge was fixed on the tensile side of the specimen to measure the uniaxial surface strain. data are recorded in a digital oscilloscope at the rate of 430 kilo samples per second. The data are filtered using CFC 1000 low pass filter to remove high frequency components. Two high-speed video cameras along with flicker free lights were used to record the fracture event. Three drop heights, namely 0.5, 1.0 and 1.5 m were used to generate an initial velocity of 3.23, 4.43 and 5.42 m/s respectively.

#### 3.2. Finite element model

Prior to experiments all specimens were CT scanned. Materialise Mimics™ was used to generate a finite element mesh (Figure 1(a)). Since optimisation methods were to be used later, the simulation time must be kept minimum. So the mid diaphysis, where the bending moment was expected to be maximum was meshed finely (Figure 1(b)). To predict bending stresses accurately it is necessary to compute the second moment of area correctly in the mid diaphysis of the long bone [5]. Since second moment of area depends on the geometry, the mid diaphysis region was meshed finely. Also since the impact happens in the mid diaphysis, to approximate Hertzian stress reasonably the mesh was made fine. Density values were mapped from Hounsfield numbers from CT scans [6, 7].

A total of 20 material sets were used. Five sets were used to represent cancellous and fifteen sets were used to represent cortical bone. Comparing the mass of FE model with the physical mass validated the model. The error was less than 2% in the eleven cases. In earlier studies conducted by the authors[8, 9] a dilatational cut-off stress[10] based failure criterion was used to predict fracture. Though the fracture patterns were predicted closely, the peak forces were over predicted. In a more recent study [11], a Von Mises plastic model with Cowper-Symonds yield stress scaling constitutive model was used. Plastic strain was used as a failure criterion. An optimisation workflow similar to the current work was used to derive material parameters. Though the structural response agreed very well with experiments, the failure of long bones was not predicted. This situation warrants the use of more realistic material models to capture yielding, damage and failure of long bones. Drucker-Prager plastic model[12] was used to capture yielding and failure in bones. As bone failure is not instantaneous but progressive. The stiffness of bone degrades gradually due to the progressive failure of collagen fibers and due to the presence of micro cracks [13]. A detailed experimental analysis [14] showed that shear damage and failure is the primary mechanism in fracture of cortical bone, hence a phenomenological damage model based on shear failure was used to capture the fracture event. Theory of the material models is not discussed here for brevity.

Density to Young's modulus relation is modeled as a bilinear curve Figure 2(a). The feasible space for the optimization routine to choose candidate variables is shown in Figure 2(b). To maintain a  $C^0$  continuity between the two lines of the bilinear model,

the intercept of the second line is assumed to be a dependent variable.

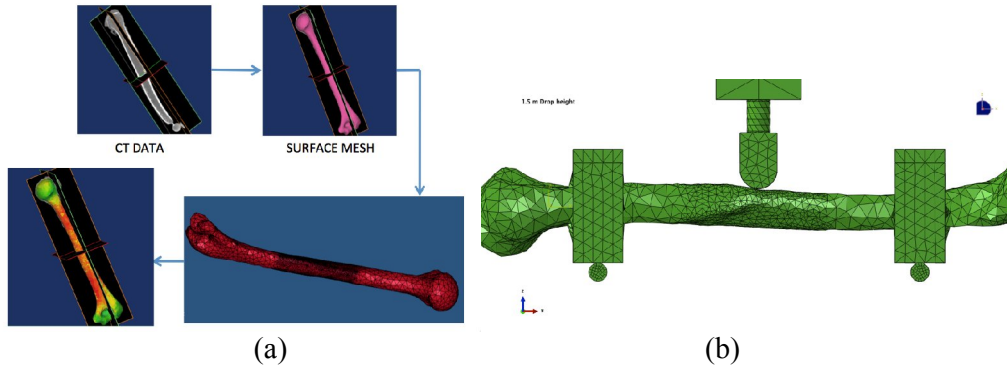


Figure 1(a) Pictorial representation of mesh generation workflow (b) Finite element mesh

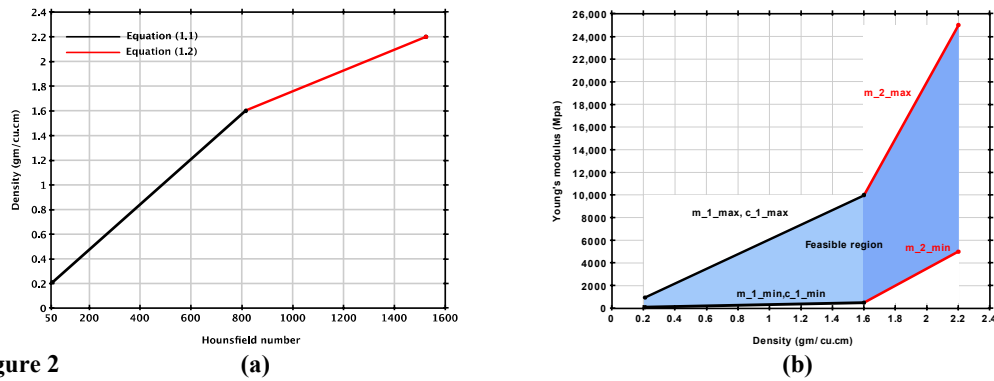


Figure 2

### 3.3. User material development

Rate dependency of elastic modulus, yielding and failure is a well-documented behavior of bone [15, 16]. These studies suggested to model elastic modulus, yielding and failure as logarithmically related to strain rate. The following relation was assumed to model the material behavior, which is similar to Johnson-Cook's

$$A_i = A_i^0 \left[ 1 + \log \left( \frac{\dot{\epsilon}}{0.001} \right) * C_i \right]$$

equation  $A_i$  and  $A_i^0$  represents the total and initial values

of the material parameters discussed above respectively,  $\dot{\epsilon}$  is the strain rate and  $C_i$  is a parameter. The reference strain rate for quasi-static response was assumed to be 0.001/s. Unfortunately a constitutive model that can take into account of this behavior is not readily available in commercial packages. Therefore a VUSDFLD subroutine was written in Abaqus/Explicit<sup>TM</sup>. Most material properties in ABAQUS/Explicit can be defined as functions of field variables,  $f_i$ . Subroutine VUSDFLD allows the user to define  $f_i$  at every integration point of an element. The subroutine has access to solution data i.e.  $f_i(\sigma, \epsilon, \epsilon_{pl}, \dot{\epsilon}; \text{etc.})$ ; therefore, the material properties can be a function of the solution data. The computed material properties inside VUSDFLD routine are then passed to the main code for stress updation. The user subroutine was validated using single element simulations. The user subroutine was compiled along with the main model. It is a good practice to compile the user subroutine as a double precision executable while using with double precision explicit solver.

### 3.4. Optimisation module

Genetic algorithm (GA) is widely used to generate best available solutions to search and optimisation problems. It uses procedures motivated by evolution such as selection, inheritance, mutation and crossover. When the solution of the problem is little known, GA can be used to extract the best available solution. For the current study an open source C++ GA code developed by Sastry and Goldberg [17] (download link in the reference) was used. In a very few studies optimization techniques were used to derive material parameters for bones under impact [18, 19]. However subject specific material assignment was done in neither of the study, however the geometry of the FE model was generated from CT scans. A schematic diagram of the workflow of the optimisation procedure is shown in Figure 3.

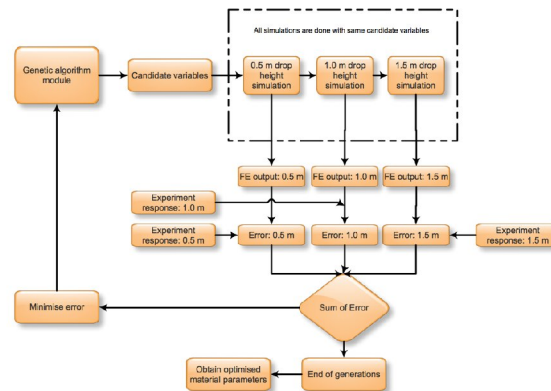


**Figure 3 Schematic diagram of the workflow of the optimisation procedure.**

## 4. RESULTS AND DISCUSSIONS

A set of material parameter was optimised by following the procedure given in Figure 3. The obtained material properties are listed in **Error! Reference source not found.** Using the obtained material parameters individual tests were simulated by developing a subject-specific finite element model and the results are plotted in Figure 4. All the simulation results agreed very well with the experimental results. Hence by capturing both the inhomogeneity using material mapping and the geometry of the specimen using the CT scan data, along with an optimisation technique; an accurate finite element model was obtained.

Sets	Bone type	Youngs Modulus (Mpa)	Yield stress (Mpa) (Tension)
1	Cancellous	734	5
2		2097	13
3		3460	21
4		4823	30
5		6186	38
6		7549	47
7		8403	52
8		9257	57
9		10111	63

10	Cortical	10945	68
11		11799	73
12		12653	78
13		13507	84
14		14361	89
15		15215	94
16		16069	100
17		16903	105
18		17757	110
19		18611	115
20		19465	121

$C_1$	Y.P	$C_2$	$\epsilon_f(\%)$	$C_3$	$u_f(\text{mm})$
0.3045	0.0062	0.18828	1.81	-0.16	0.24

**Table 1 Optimised parameters**

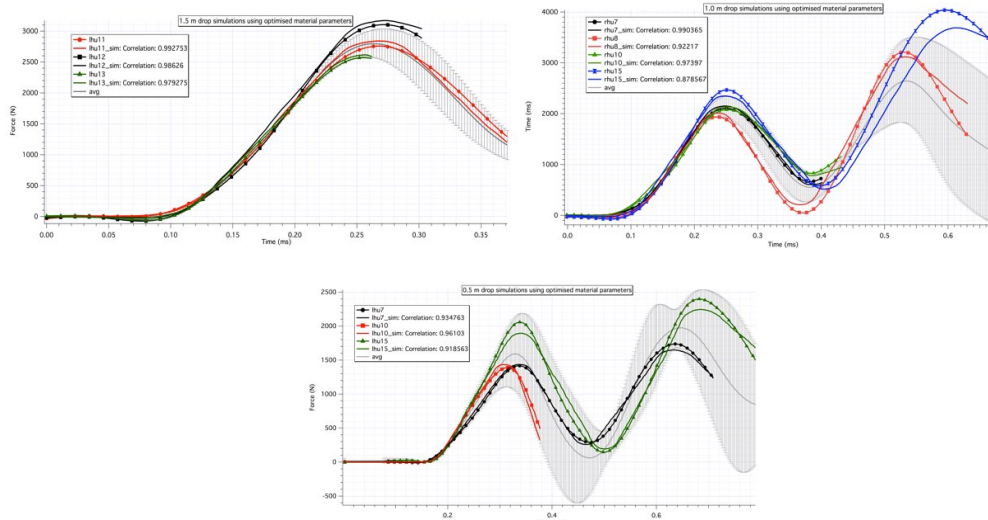


**Figure 4 Finite element simulations with optimised material properties**

**Fracture types from experiments and simulation**

Eleven fractures were oblique and one fracture was transverse in nature. Eight of the oblique fractures were of the pattern as shown in Figure 5(a), where there is a crack diversion in the compression side of impact. These fractures are observed only in 1.5 m and 1.0 m drop experiments. The other three were of the pattern as shown in Figure 5(b), where there is no crack diversion in the compression side of impact. This pattern is observed only in 0.5 m drop tests.



**Figure 5 Fracture types observed in experiments. Each black rectangle is 20 mm.**

**Error! Reference source not found.** shows the comparison between high-speed video and simulation results on selected frames for the most frequently occurs fracture type.

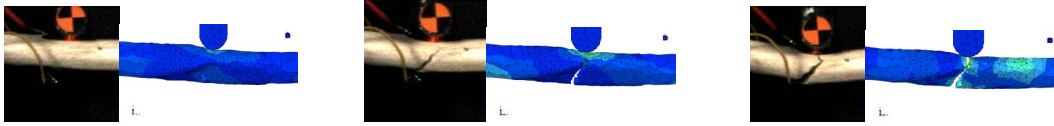


**Figure 6 Comparison between high-speed video frame and simulation. (a) At time  $t=0.26$  ms: Fracture initiation in lhu13. (b) At time  $t=0.37$  ms (c) At time  $t=1.1$  ms**

The fracture type that was observed in 0.5 m drop experiments is shown in **Error! Reference source not found.**. The main difference between this fracture and the one observed in 1.5 m and 1.0 m drop experiments is that there is no crack diversion seen in the concave (compression) side.



**Figure 7 Fracture type observed in 0.5 m drop experiments**

## 5. CONCLUSION

Currently there are no finite element material models for bones, which can predict both force response as well as fracture types. However models based on critical plastic strain have been used in human body finite element models, which can predict force response but not fracture details [3, 20]. In this study a methodology was presented which utilized experimental observations, subject specific material mapping, subject specific geometry generation and optimisation tools to derive a single material model for a wide range of strain rates.

## 6. REFERENCES

1. Kress TA, Porta DJ: **Characterization of Leg Injuries from Motor Vehicle Impacts**. In: *17th International Technical Conference on the Enhanced Safety of Vehicles (ESV): 2001; Amsterdam*.
2. Mertz HJ: **Anthropomorphic Test Devices**. In: *Accidental injury: biomechanics and prevention*. Edited by Nahum AM, Melvin J: Springer; 2002: 637.
3. Takahashi Y, Kikuchi Y, Konosu A, Ishikawa H: **Development and Validation of the Finite Element Model for the Human Lower Limb of Pedestrians**. In: *44th Stapp Car Crash Conference*. 2000.
4. Hill K: **Contribution of the Motor Vehicle Supplier Sector to the Economies of the United States and its 50 States**. In.: Research Triangle Park, NC: The Motor & Equipment Manufacturers Association; 2007.
5. O'Neill MC, Ruff CB: **Estimating human long bone cross-sectional geometric properties: a comparison of noninvasive methods**. *J Hum Evol* 2004, **47**(4):221-235.
6. Esses SI, Lotz JC, Hayes WC: **Biomechanical properties of the proximal femur determined in vitro by single-energy quantitative computed tomography**. *Journal of Bone and Mineral Research* 1989, **4**(5):715-722.
7. Harp JH, Aronson J, Hollis M: **Noninvasive determination of bone stiffness**

- for distraction osteogenesis by quantitative computed tomography scans.** *Clin Orthop Relat Res* 1994(301):42-48.
8. Arun M, Mukherjee S, Chawla A: **Reconstructing fracture progression in impact.** In: *Expert Symposium on Accident Research; Hannover.* 2010.
  9. Chawla A, Mukherjee S, Arun M: **Predicting fractures in human bones under impact.** In: *6th World congress of biomechanics: 2010; Singapore.* 2010: 294.
  10. Al-Hassani STS, Chen D, Sarumi M: **A simple non-local spallation failure model.** *International Journal of Impact Engineering* 1997, **19**(5-6):493-501.
  11. Sudipto M, Anoop C, Saurabh H, Debashish S, Arun MWJ: **Dynamic properties of the shoulder complex bones.** In: *Society of Automotive Engineers.* 2011.
  12. Drucker DC, Prager W: **Soil mechanics and plastic analysis for limit design.** *Quarterly of Applied Mathematics* 1952, **10**(2):8.
  13. Nalla RK, Kruzic JJ, Kinney JH, Ritchie RO: **Mechanistic aspects of fracture and R-curve behavior in human cortical bone.** *Biomaterials* 2005, **26**(2):217-231.
  14. Ebacher V, Wang R: **A Unique Microcracking Process Associated with the Inelastic Deformation of Haversian Bone.** *Advanced Functional Materials* 2009, **19**(1):57-66.
  15. McElhaney JH: **Dynamic response of bone and muscle tissue.** *Journal of applied physiology* 1966, **21**(4):1231-1236.
  16. Wood JL: **Dynamic response of human cranial bone.** *Journal of Biomechanics* 1971, **4**(1):1-2, IN1-IN3, 3-12.
  17. **Single and Multiobjective Genetic Algorithm Toolbox in C++** [<http://illigal.org/category/source-code/>]
  18. Kim J-E, Li Z, Ito Y, Huber CD, Shih AM, Eberhardt AW, Yang KH, King AI, Soni BK: **Finite element model development of a child pelvis with optimization-based material identification.** *Journal of Biomechanics* 2009, **42**(13):2191-2195.
  19. Untaroiu, Crandall: **Parameter Identification and Sensitivity Analysis of Cortical Bone Material Models using Finite Element Optimization Techniques.** In: *ASME Summer Bioengineering Conference; Amelia Island, FL.* 2006.
  20. Untaroiu CD: **Development and validation of a finite element model of human lower limb.** University of Virginia; 2005.